Peripheral cannabinoid receptor, CB2, regulates bone mass

Orr Ofek*, Meliha Karsak†, Nathalie Leclerc‡, Meirav Fogel*, Baruch Frenkel‡, Karen Wright§, Joseph Tam*, Malka Attar-Namdar*, Vardit Kram*, Esther Shohami¶, Raphael Mechoulam‖, Andreas Zimmer†, and Itai Bab*,**

*Bone Laboratory and Departments of ¶Pharmacology and ‖Medicinal Chemistry and Natural Products, Hebrew University of Jerusalem, Jerusalem 91120, Israel; †Department of Psychiatry, Life and Brain Center, University of Bonn, 53105 Bonn, Germany; ‡Department of Orthopaedic Surgery, Institute for Genetic Medicine, University of Southern California Keck School of Medicine, Los Angeles, CA 90033; and §Department of Pharmacology, University of Bath, Bath BA2 7AY, United Kingdom

Edited by Hector F. DeLuca, University of Wisconsin, Madison, WI, and approved November 11, 2005 (received for review May 22, 2005)

The endogenous cannabinoids bind to and activate two G protein-coupled receptors, the predominantly central cannabinoid receptor type 1 (CB1) and peripheral cannabinoid receptor type 2 (CB2). Whereas CB1 mediates the cannabinoid psychotropic, analgesic, and orectic effects, CB2 has been implicated recently in the regulation of liver fibrosis and atherosclerosis. Here we show that CB2-deficient mice have a markedly accelerated age-related trabecular bone loss and cortical expansion, although cortical thickness remains unaltered. These changes are reminiscent of human osteoporosis and may result from differential regulation of trabecular and cortical bone remodeling. The *CB2*$^{-/-}$ phenotype is also characterized by increased activity of trabecular osteoblasts (bone-forming cells), increased osteoclast (the bone-resorbing cell) number, and a markedly decreased number of diaphyseal osteoblast precursors. CB2 is expressed in osteoblasts, osteocytes, and osteoclasts. A CB2-specific agonist that does not have any psychotropic effects enhances endocortical osteoblast number and activity and restrains trabecular osteoclastogenesis, apparently by inhibiting proliferation of osteoclast precursors and receptor activator of NF-κB ligand expression in bone marrow-derived osteoblasts/stromal cells. The same agonist attenuates ovariectomy-induced bone loss and markedly stimulates cortical thickness through the respective suppression of osteoclast number and stimulation of endocortical bone formation. These results demonstrate that the endocannabinoid system is essential for the maintenance of normal bone mass by osteoblastic and osteoclastic CB2 signaling. Hence, CB2 offers a molecular target for the diagnosis and treatment of osteoporosis, the most prevalent degenerative disease in developed countries.

bone remodeling | HU-308 | osteoblast | osteoclast

The endogenous cannabinoids bind to and activate the cannabinoid receptors 1 and 2 (CB1 and CB2, respectively). Both are seven-transmembrane domain receptors, and they share 44% identity. They are coupled to the inhibitory guanine nucleotide-binding regulatory protein subclass of G proteins and inhibit stimulated adenylyl cyclase activity (1). That CB1 and CB2 are not functionally identical is demonstrated by the selective regulation of ion channels by only CB1 (2). CB1 is present in the brain and in peripheral neurons and accounts for most of the actions of cannabinoid drugs and endocannabinoids on the central nervous system (3, 4). CB2 was reported in the immune system (5), in liver cirrhosis (6), and in atherosclerotic plaques (7).

In vertebrates, bone mass and shape are determined by continuous remodeling consisting of the concerted and balanced action of osteoclasts, the bone-resorbing cells, and osteoblasts, the bone-forming cells. Osteoporosis, the most prevalent degenerative disease in developed countries, results from the impairment of this balance, leading to bone loss and increased fracture risk. It has been recently reported that bone remodeling is subject to central control through pathways that involve signaling by the hypothalamic receptors for leptin and neuropeptide Y (8, 9), which are also associated with the regulation of endocannabinoid brain levels (10). These observations led us to assess the role of the endocannabinoid signaling system in the regulation of bone mass. Indeed, we demonstrate here a low bone mass phenotype in mice deficient for the peripheral cannabinoid receptor (CB2), which is normally expressed in osteoblasts, osteoclasts, and their precursors. A CB2-specific agonist, which has no psychotropic or other central effects, regulates the activity of these cells and attenuates ovariectomy (OVX)-induced bone loss. These data suggest an important regulatory role of the endocannabinoid system in bone and offer molecular targets for the development of diagnostic and therapeutic approaches to osteoporosis.

Results

Low Bone Mass Phenotype and High Bone Turnover in CB2$^{-/-}$ Mice. *CB2*$^{-/-}$ mice are healthy, fertile, and of size and weight indistinguishable from their age-matched WT controls (11). Indeed, we could not find any overt phenotype in our previous analysis of *CB2*-knockout mice, and thus the function of the CB2 receptor remained obscure. The present skeletal analysis shows a low bone mass phenotype in both male and female *CB2*$^{-/-}$ mice (Fig. 1; see also Fig. 7, which is published as supporting information on the PNAS web site). In females, the trabecular bone volume density (BV/TV) was significantly decreased already at the age of 8 weeks (Fig. 7*A*). The trabecular number (Tb.N) at this age was lower in both males and females (Figs. 1*C* and 7*B*). The findings in 1-year-old male mice indicate progressive, marked trabecular bone loss with transition from plate- to rod-like trabecular structure (Fig. 1*A*), reportedly associated with a net increase in bone resorption (12). The BV/TV and Tb.N in these animals were approximately half compared with age-matched WT controls (Fig. 1 *B* and *C*). Bone histomorphometric measurements were carried out in the 8-week-old females. These results show that the osteoclast number per bone surface area was almost 40% higher in the *CB2*$^{-/-}$ mice (Fig. 7*C*). Mineral appositional rate and bone formation rate were increased by ≈20% (Fig. 7 *D* and *E*). Together these data indicate that the low bone mass in *CB2*$^{-/-}$ mice is associated with high bone turnover, as observed, for example, in postmenopausal osteoporosis, where the increase in bone formation is insufficient to compensate for the strongly stimulated bone resorption. Another

Conflict of interest statement: Rights pertinent to HU-308 are owned by Yissum Research Development Company of the Hebrew University of Jerusalem and have been licensed to Pharmos, Ltd., Rehovot, Israel.

This paper was submitted directly (Track II) to the PNAS office.

Abbreviations: CB1, cannabinoid receptor type 1; CB2, cannabinoid receptor type 2; CFU-OB, colony-forming unit osteoblastic; M-CSF, macrophage colony-stimulating factor; μCT, microcomputed tomographic; NeMCO, newborn mouse calvarial osteoblasts; OVX, ovariectomy or ovariectomized; RANKL, receptor activator of NF-κB ligand; TNSALP, tissue nonspecific alkaline phosphatase; TRAP, tartrate-resistant acid phosphatase.

**To whom correspondence should be addressed at: Bone Laboratory, Hebrew University of Jerusalem, P.O.B. 12272, Jerusalem 91120, Israel. E-mail: babi@cc.huji.ac.il.

www.pnas.org/cgi/doi/10.1073/pnas.0504187103

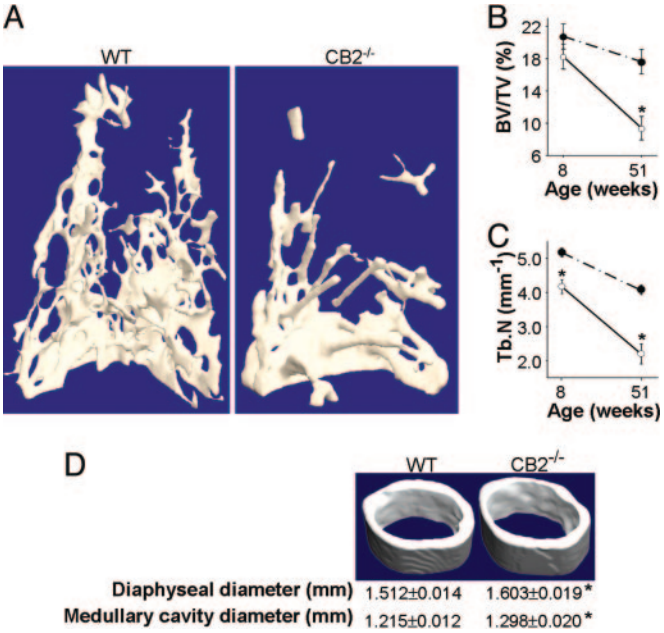

Fig. 1. Low trabecular bone mass and cortical expansion in $CB2^{-/-}$ mice. (*A–C*) Distal femoral metaphysis. (*A*) 3D trabecular bone structure in 51-week-old mice. (*B*) Trabecular bone volume density as percent trabecular network of total metaphyseal volume (BV/TV). (*C*) Trabecular number per millimeter metaphyseal line (Tb.N). Open circles, $CB2^{-/-}$ mice; filled circles, WT mice. (*D*) Femoral mid-diaphysis of 8-week-old mice. Microcomputed tomographic (μCT) analysis in male mice. Quantitative data are mean ± SE. *, $P < 0.05$.

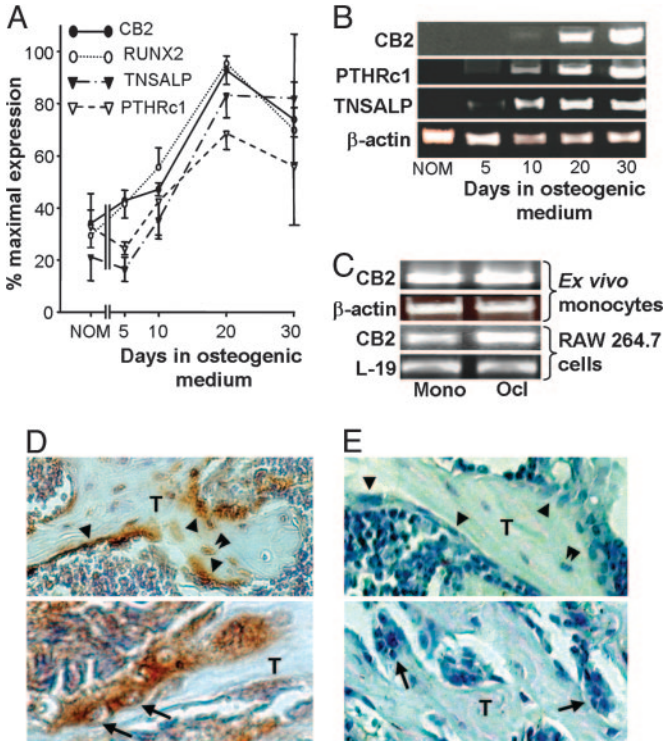

Fig. 2. CB2 expression in normal bone. (*A*) Real-time RT-PCR of CB2 and osteoblast differentiation markers in bone marrow-derived primary stromal cell cultures undergoing osteoblastic differentiation in osteogenic medium. NOM, cells grown for 20 days in nonosteogenic medium; RUNX2, runt-related transcription factor 2; TNSALP, tissue nonspecific alkaline phosphatase. (*B*) RT-PCR analysis in MC3T3 E1 osteoblastic cell line grown in osteogenic medium. PTHRc1, parathyroid hormone (PTH)/PTH-related protein receptor 1. (*C*) RT-PCR analysis in primary culture of monocytic cells undergoing osteoclastogenesis. Upper lanes, bone marrow-derived culture grown in the presence of M-CSF and RANKL; lower lanes, RAW 264.7 cells grown with RANKL; Mono, undifferentiated monocytes; Ocl, osteoclast-like, tartrate-resistant acid phosphatase (TRAP)-positive multinucleated cells. (*D* and *E*) Immunohistochemical localization of CB2-positive osteoblasts (arrowheads), osteocytes (double arrowhead), and osteoclasts (arrows) in distal femoral metaphysis of WT mice (*D*) but not of $CB2^{-/-}$ mice (*E*).

feature reminiscent of human osteoporosis is that the decreased trabecular bone mass is associated with cortical expansion (13), consisting of increased total diaphyseal and medullary cavity diameters and preservation of cortical thickness (Figs. 1*D* and 7*F*).

Expression of Cannabinoid Receptors in Osteoblasts and Osteoclasts. To explore the mechanism involved in the effect of CB2 signaling in bone, we initially analyzed cannabinoid receptor expression in mouse diaphyseal bone marrow-derived stromal cells grown in osteogenic medium (14). Real-time RT-PCR demonstrated progressive expression of CB2 mRNA, which paralleled the expression of the osteoblastic marker genes *TNSALP* (encoding tissue nonspecific alkaline phosphatase) and *RUNX2* (15). CB2 mRNA levels were much lower when the same cultures were propagated in nonosteogenic medium (Fig. 2*A*). CB2 was also progressively expressed in MC3T3 E1 osteoblastic cells cultured in osteogenic medium (Fig. 2*B*). CB1 mRNA was extremely low in either culture system (data not shown).

We next measured CB2 expression during *in vitro* osteoclastogenesis in bone marrow-derived primary monocytic cultures. Expression of CB2 in the monocyte-macrophage lineage had been reported in refs. 16 and 17. As shown in Fig. 2*C*, CB2 was expressed in bone marrow-derived osteoclasts formed in the presence of macrophage colony-stimulating factor (M-CSF) and receptor activator of NF-κB ligand (RANKL) and in their monocytic progenitors (Fig. 2*C*). RAW 264.7-derived osteoclast-like cells also expressed CB2 mRNA (Fig. 2*C*). As in the case of the osteoblastic cells, CB1 mRNA was undetectable in the osteoclast-like cells and in their progenitors (data not shown).

To address CB2 expression in bone *in vivo*, immunohistochemical analysis was performed on distal femoral metaphyseal sections. As shown in Fig. 2*D*, CB2 receptors are clearly expressed in osteoblasts, osteocytes, and osteoclasts of WT, but not $CB2^{-/-}$ mice (Fig. 2*E*).

Role of CB2 Signaling in Osteoblastic Cells. Expression of the CB2 receptor in bone cells suggested that CB2 ligands could exert their skeletal effect in a cell-autonomous manner. We therefore tested the effects of HU-308, a synthetic, highly specific, small molecule CB2 agonist (18) (see Fig. 8*A*, which is published as supporting information on the PNAS web site), in primary osteoblastogenic culture of bone marrow-derived stromal cells. HU-308 potently increased the number of the WT-derived differentiating stromal cells, with maximal 205% stimulation at 10^{-8} M and $EC_{50} = 0.35$ nM. HU-308 did not affect similarly treated cells obtained from $CB2^{-/-}$ mice (Fig. 3*A*). Noladin ether, a specific CB1 agonist (19) had no significant effect (Fig. 8*B*). At this early differentiation stage, TNSALP activity and matrix mineralization were unaffected by the CB2 ligand (data not shown). Thus, the HU-308-induced increase in cell number in this system is consistent with a CB2-mediated stimulation of preosteoblastic cell pool expansion as a mechanistic aspect of the endocannabinoid action in bone. Colony-forming unit osteoblastic (CFU-OB) formation was used to study the role of CB2 signaling on terminal osteogenic differentiation of the bone marrow-derived stromal cells. The CFU-OB counts were markedly decreased in the $CB2^{-/-}$ mice compared with WT cultures (Fig. 3*B*). HU-308 increased the CFU-OB counts in cultures from WT mice. Jointly, these data suggest that CB2 signaling regulates the supply of diaphyseal endocortical osteoblasts, and that undersupply

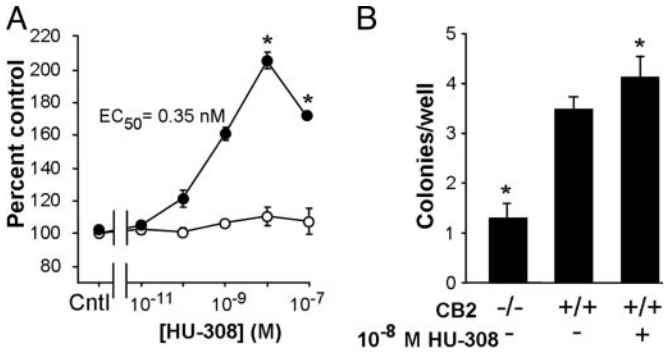

Fig. 3. CB2 signaling regulates supply of diaphyseal osteoblasts. (*A*) CB2-specific agonist HU-308 stimulates the number of diaphyseal-derived bone marrow stromal cells. Cells were grown for 10 days in osteogenic medium followed by a 48-h challenge with HU-308 (see further details in *Methods*). Filled circles, cells derived from WT mice; open circles, cells derived from $CB2^{-/-}$ mice. Data are mean ± SE obtained in triplicate culture wells per condition. (*B*) *Ex vivo* regulation of bone marrow-derived CFU-OB by $CB2^{-/-}$ signaling. Data are mean ± SE obtained in five $CB2^{-/-}$ and four WT mice per condition (10 wells per mouse). *, $P < 0.05$.

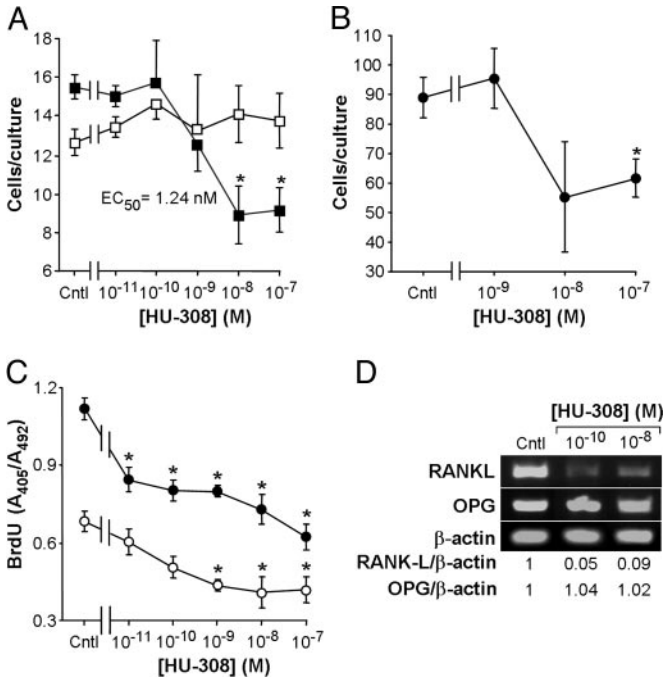

Fig. 5. CB2-specific agonist, HU-308, restrains osteoclastogenesis. (*A*) Number of TRAP-positive multinucleated cells in primary bone marrow-derived monocyte culture from WT (filled squares) and $CB2^{-/-}$ (open squares) mice maintained for 6 days in osteoclastogenic conditions (M-CSF and RANKL) with the indicated HU-308 concentrations. Cntl, control without HU-308. Data are mean ± SE obtained in 24 culture wells per condition. (*B*) Number of TRAP-positive multinucleated cells in RAW 264.7 cell cultures incubated for 7 days with RANKL and the indicated HU-308 concentrations. (*C*) DNA synthesis in RAW 264.7 cultured for 3 days with (open circles) or without (filled circles) RANKL and HU-308 as indicated. Data in *B* and *C* are mean ± SE obtained in triplicate culture wells per condition. (*D*) RT-PCR analysis of RANKL and osteoprotegerin (OPG) expression in bone marrow-derived primary stromal cell cultures. Cells from WT mice were incubated for 10 days in osteogenic medium and then challenged for 8 h with HU-308 or control (Cntl) medium. *, $P < 0.05$.

of committed osteogenic precursors is the cause of decreased endocortical bone formation that contributes to the cortical expansion in the CB2-null mice.

Because bone marrow-derived primary stromal cell cultures are nonhomogenous, we further tested the effect of HU-308 on cell proliferation and osteogenic functions in primary newborn mouse calvarial osteoblasts (NeMCO) cells and the MC3T3 E1 osteoblastic cell line. As in the stromal cell osteoblastogenic culture, we found that HU-308 stimulated proliferation measured as both increased BrdUrd incorporation into newly synthesized DNA and DNA content (Fig. 4*A*; see also Fig. 9 *A* and *B*, which is published as supporting information on the PNAS web site). The stimulation of DNA synthesis was blocked by pertussis toxin (Fig. 9*A*), consistent with the notion that the HU-308 mitogenic activity engages CB2 signaling by an inhibitory $G_{i/o}$ protein (20). The mitogenic activity of HU-308 in the NeMCO and MC3T3 E1 models was accompanied by enhancement of the osteoblast phenotype; the respective TNSALP activity was increased in these systems by 60% and 75% (Figs. 4*B* and 9*C*), and the accumulation of extracellular mineral, an ultimate osteoblastic function, showed multiple-fold enhancement (Figs. 4*C* and 9*D*). As in the case of the bone marrow-derived stromal cells, NeMCO cells from $CB2^{-/-}$ mice showed no response to HU-308 (Fig. 4). Together, the decrease in CFU-OB derived from the $CB2^{-/-}$ mice and HU-308-induced stimulation of CFU-OB obtained from WT mice and enhancement of NeMCO and MC3T3 E1 cell function suggest that CB2 signaling in osteoblasts is cell autonomous and independent of the presence of osteoclasts or their precursors.

CB2 Signaling Mitigates Osteoclastogenesis. HU-308 also had a cell-autonomous effect in bone marrow-derived primary monocytic cultures undergoing osteoclastic differentiation under the influence of M-CSF and RANKL. In cultures derived from WT, but not $CB2^{-/-}$ mice, HU-308 dose-dependently suppressed the formation of osteoclast-like cells, with maximal 42% inhibition at 10^{-8} M and EC_{50} = 1.24 nM (Fig. 5*A*). HU-308 also decreased the number of osteoclast-like cells formed in a 7-day RAW 264.7 cell culture supplemented with RANKL. Maximal suppression in this system was 40% at 10^{-8} M (Fig. 5*B*). To test whether this suppression of osteoclastogenesis resulted from an antimitogenic effect in preosteoclasts, we analyzed DNA synthesis in RAW 264.7 cells grown for 3 days with or without RANKL. Regardless of the presence of RANKL, HU-308 inhibited BrdUrd incorporation in these cells, also with a maximal 40% effect (Fig. 5*C*). Thus, whereas HU-308 is mitogenic in the osteoblast lineage, it is antimitogenic in the monocytic–osteoclastic lineage. HU-308 also markedly reduced

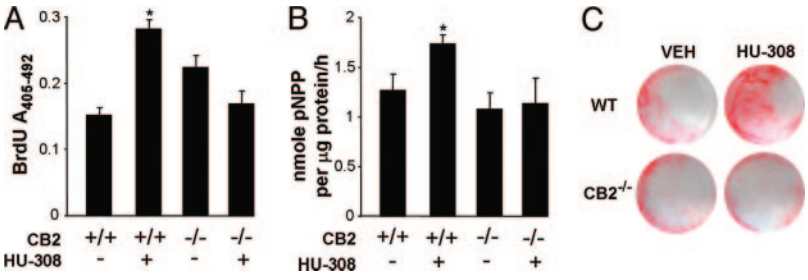

Fig. 4. CB2-specific agonist stimulates growth and differentiation of newborn calvarial osteoblasts derived from WT but not from $CB2^{-/-}$ mice. Cells were grown for 12 days in osteogenic medium before challenging with 10^{-8} M HU-308. (*A*) DNA synthesis. (*B*) TNSALP activity. pNPP, *p*-nitrophenyl phosphate. (*C*) Mineral staining with alizarin red S. Cells were treated with HU-308 for 48 h in *A* and 10 days in *B* and *C*. Data in *A* and *B* are mean ± SE obtained in 12 and 3 culture wells per condition, respectively. Images in *C* are representative of 3–6 wells per condition. *, $P < 0.05$.

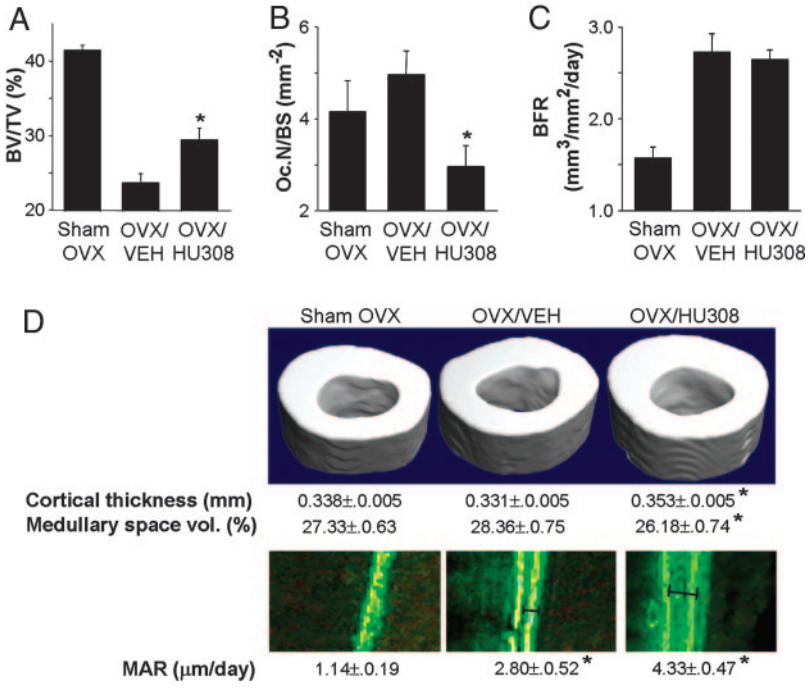

Fig. 6. CB2-specific agonist, HU-308, attenuates OVX-induced femoral bone loss in sexually mature C3H mice. A 4-week treatment with HU-308 at 10 mg/kg per day commenced at the time of OVX. (*A*) μCT analysis of trabecular bone volume density. (*B*) Histomorphometric analysis of osteoclast number per bone surface area (Oc.N/BS). (*C*) Histomorphometric analysis of bone formation rate (BFR). *A–C* were analyzed in the distal femoral metaphysis. (*D*) Mid-diaphyseal μCT (*Upper*) and histomorphometric (*Lower*) analyses. Quantitative microtomograpic and histomorphometric parameters are as defined in Fig. 1. Data are mean ± SE. *, $P < 0.05$.

RANKL mRNA in bone marrow stromal cells undergoing osteoblastic differentiation, leaving osteoprotegerin expression unaffected (Fig. 5*D*). Selective regulation of RANKL has been reported in ref. 21; the present reduction in RANKL expression could contribute to the *in vivo* inhibition of osteoclast number seen in HU-308-treated OVX mice (Fig. 6*B*). A qualitative assessment suggested that HU-308 did not affect osteoclast size or the number of osteoclast nuclei (data not shown).

The lack of response to HU-308 in all culture systems derived from *CB2*$^{-/-}$ mice clearly demonstrates that this ligand not only has great preference for CB2 over CB1 receptors, but also that it does not act on noncannabinoid receptors.

Attenuation of OVX-Induced Bone Loss by HU-308. In view of the antiosteoclastic and proosteoblastic activities of HU-308 *in vitro*, and because it is nonpsychotropic (18), CB2-specific ligands such as HU-308 could provide an opportunity to augment bone mass while avoiding the cannabinoid psychotropic activity. We therefore tested the antiosteoporotic potential of HU-308 in an OVX C3H mouse model of postmenopausal osteoporosis. Indeed, whereas OVX induced 41% trabecular bone loss in untreated mice, HU-308 attenuated this loss to only 27% (Fig. 6*A*). The protective effect of HU-308 was attributable to reduction in the osteoclast number to levels lower than those measured in OVX and even sham-operated mice (Fig. 6*B*). In the trabecular compartment, HU-308 did not stimulate bone formation, which was already enhanced as part of the high bone turnover triggered by OVX (Fig. 6*C*) (22). By contrast, HU-308 induced a marked increase in the cortical thickness, which exceeded the thickness in either OVX or sham-OVX mice (Fig. 6*D Upper*). This increase was associated with a significant reduction in the size of the medullary cavity (Fig. 6*D Upper*), which could be accounted for by the stimulation of endocortical bone formation (Fig. 6*D Lower*). Thus, treatment with a CB2 agonist can oppose bone weakening after loss of estrogen by concomitantly attenuating osteoclast-mediated bone resorption (Figs. 5 and 6*B*) and stimulating osteoblast-mediated bone formation (Figs. 3, 4, and 6*D*).

Discussion

Our analyses demonstrate that the endocannabinoid system regulates bone mass by signaling via the peripheral CB2 expressed in bone. Specifically, we show that CB2-deficient mice have a low bone mass phenotype, suggesting that endocannabinoids play an essential role in the maintenance of bone mass by signaling through CB2. We further show that these receptors are expressed in cells of both the osteoblast and osteoclast lineages and that exposure of these cells to a CB2-specific agonist results in distinct responses, suggesting that CB2 signaling contributes to the maintenance of bone mass by two mechanisms: (*i*) direct stimulation of stromal cells/osteoblasts; and (*ii*) inhibition of monocytes/osteoclasts, both directly and by inhibition of osteoblast/stromal cell RANKL expression. We then demonstrate the feasibility of designing a cannabinoid-based, antiosteoporotic therapy that is free of psychotropic effects.

CB2 is expressed in the vast majority of hematopoietic cells, including macrophages, and attenuates immune responses (17, 19, 23, 24). In line with these reports, we found here that osteoclasts, cells derived from the monocyte–macrophage lineage (25), have high levels of CB2 mRNA and are more abundant in the CB2-deficient mice. Moreover, treatment with HU-308, a specific CB2 agonist (18), suppresses osteoclastogenesis in WT OVX animals, apparently by a mechanism that involves CB2-mediated mitogenic inhibition of osteoclast precursors. That this inhibition directly involves the osteoclast lineage is proposed by the restrained osteoclastogenesis in the homogenous RAW 264.7 cell line. We also show that HU-308 inhibits RANKL expression in stromal cells/osteoblasts, suggesting an additional *in vivo* mechanism whereby CB2 signaling restrains osteoclastogenesis by reducing the availability of RANKL, which is a critical osteoclastogenic factor (25). Regulation of osteoclastogenesis, both by direct action on cells of the osteoclast lineage and indirectly by stromal cells/osteoblasts has been reported recently in the cases of the sympathetic nervous system (26), tumor necrosis factor (TNF), and interleukin 1 (IL-1) (27). Jointly, these data suggest that physiologic CB2 signaling exerts tonic repression of osteoclastogenesis. Interestingly, it has been recently reported that CB2 antagonists inhibit osteoclastogenesis *in vitro*, implying that CB2 signaling promotes osteoclast differentiation and function (28), the opposite of the conclusion from this article. A possible explanation for this discrepancy is that the effect of CB2 ligands is concentration-dependent inasmuch as the effect of HU-308 on osteoclastogenesis is seen at concentrations

2–3 orders of magnitude lower compared with the effective antagonist dose.

Although we show direct effects of CB2 signaling on osteogenesis and osteoclastogenesis, the skeletal effects of HU-308 could involve CB2 receptors in nonskeletal cells. For example, in cells of the monocyte/macrophage system, CB2 signaling inhibits the expression of proresorptive cytokines, such as TNF and IL-1 (29). Interestingly, CB2 activation stimulates the expression of IL-1 receptor antagonist (30), which is normally present in bone (31) and suppresses osteoclast formation (32). In addition, endocannabinoids enhance nitric oxide (NO) synthase activity and NO release from monocytes and mast cells (33, 34). NO inhibits bone formation and resorption (35), and therefore this endocannabinoid activity is consistent with the CB2-mediated suppression of bone remodeling implied by the high bone turnover in the CB2-null mice.

Increased bone resorption in the $CB2^{-/-}$ mice could be expected to result in a compensatory increase in bone formation (36). The failure of osteoblasts to fully balance the increase in bone resorption can be explained by a requirement for CB2 signaling in osteoblast growth and differentiation. Indeed, we show that CB2 expression in differentiating osteoblasts progressively increases, paralleling the increasing expression of the osteoblastic markers TNSALP, PTHRc1, and RUNX2, a master osteogenic transcription factor (15). We further demonstrate that the expression of CB2 is essential for the physiologic supply of osteoblasts, at least in the endocortical diaphyseal compartment.

That HU-308 prevented OVX-induced trabecular bone loss only partially is possibly attributable to the failure of this CB2 agonist to stimulate trabecular bone formation in the OVX mice. It seems that the HU-308-activated CB2 signaling targets a bone anabolic mechanism, which is saturated in the OVX animals because of their high bone turnover during the treatment period. Jointly, the data in $CB2^{-/-}$ mice and HU-308-treated *ex vivo* cultures and OVX animals suggest that the main effects of CB2 in the trabecular and cortical compartments are the inhibition of bone resorption and stimulation of endocortical bone formation, respectively. Indeed, trabecular and cortical bone cells may respond differently to activation of the same receptors, as exemplified by the cases of PTH receptor 1 (PTHRc1) and androgen receptor (37, 38). Still, further investigation is required to fully understand the processes involved in this differential regulation, in particular the role of cannabinoids in endocortical bone resorption and periosteal bone growth, which, like endosteal bone formation, also determine radial bone growth, cortical thickness, and cortical expansion.

Adult bone mass is affected by the accrual of peak bone mass and its later maintenance by balanced remodeling (39). The almost normal bone mass in 8-week-old $CB2^{-/-}$ mice compared with the vast bone loss observed by 1 year of age suggests a differential role for CB2 in balancing bone remodeling. Does CB2 signaling operate in humans as it does in mice? We have recently reported an association of polymorphism in the human gene encoding CB2 with postmenopausal osteoporosis (40). Bone density studies in well defined cohorts of chronic marijuana users (41) to establish the role of CB2 signaling in human bone metabolism are also advocated. Finally, duplication in humans of our results demonstrating inhibition of osteoclast number and stimulation of bone formation in OVX mice by a synthetic cannabinoid will provide unprecedented opportunities for the design of a single, orally available antiosteoporotic therapy that is concomitantly anabolic and antiresorptive. That the specificity of this synthetic agonist is for the CB2 implies the absence of undesirable psychotropic effects shared by many of the nonspecific cannabinoid receptor ligands that, in addition to CB2, activate the neuronal CB1.

Methods

Animals. Mice with a deletion of the *CNR2* gene ($CB2^{-/-}$ mice) (11) were crossed for 10 generations to WT C57BL/6J mice to generate a congenic C57BL/6J $CB2^{-/-}$ strain. The effect of CB2 signaling on OVX-induced bone loss was analyzed in normal C3H mice (Harlan) because of their high femoral bone density (42), which allows for a substantial amount of bone loss to occur. Because of the low trabecular bone volume density in C57BL/6J females (Fig. 7*A*), the absolute amount of OVX-induced bone loss in these animals is small, and a large sample is required to achieve statistical significance. Also, the number of calcein-labeled packets (see *Results*) in OVX C57BL/6J mice is often too small for the calculation of bone formation parameters in the trabecular compartment. HU-308, a synthetic CB2-specific agonist with a molecular weight of 414, was prepared as described in ref. 18 and injected i.p. into OVX and control mice once daily as ethanol/emulphor/saline (1:1:18) solution. To study bone formation, newly formed bone was vitally labeled in all reported animals by the fluorochrome calcein (Sigma), injected i.p. (15 mg/kg) 4 days and 1 day before euthanization. Groups of 8–10 mice, ages 8–11 or 51 weeks, were used in each experiment. The experimental protocols were approved by the Institutional Animal Care and Use Committee, Faculty of Medicine, Hebrew University of Jerusalem and by the Regierungspräsidium Köln for the University of Bonn.

Microcomputed Tomographic (μCT) Analysis. Whole femora were examined by a μCT system (μCT 40, SCANCO Medical, Bassersdorf, Switzerland) equipped with a 5-μm focal spot microfocus x-ray tube as a source. A 2D charge-coupled device, coupled to a thin scintillator as a detector, permitted parallel acquisition of stacks, including 20 tomographic images. The long axis of the femur was set parallel to the plane of the x-ray beam axis. The x-ray tube was operated at 50 kV (kilovolt) and 160 μA. The integration time was set to 100 ms. The scans were performed at a resolution of 20 μm in all three spatial dimensions (medium-resolution mode). 2D computed tomographic images were reconstructed in $1,024 \times 1,024$ pixel matrices from 1,000 projections by using a standard convolution backprojection procedure with a Shepp and Logan filter. Images were stored in 3D arrays with an isotropic voxel size of 20 μm. A constrained 3D Gaussian filter (width, $\sigma = 0.8$; support, 1 voxel width) was used partly to suppress the noise in the volumes. The samples were binarized by using a global thresholding procedure (43). The threshold was set to 22.4% and 16.0% of the maximal gray-scale value for cortical bone and trabecular bone, respectively. Morphometric parameters were determined by using a direct 3D approach (44). Trabecular bone parameters were measured in a metaphyseal segment, extending proximally from the proximal tip of the primary spongiosa to the proximal border of the distal femoral quartile. Cortical bone parameters were determined in a diaphyseal segment extending 1.12 mm distally from the midpoint between the femoral ends.

Histomorphometry and Immunohistochemistry. After μCT image acquisition, the specimens were embedded undecalcified in Technovit 9100 (Heraeus). Longitudinal sections through the midfrontal plane were left unstained for dynamic histomorphometry based on the vital calcein double labeling. To identify osteoclasts, consecutive sections were stained for tartrate-resistant acid phosphatase (TRAP) (45). Parameters were determined according to a standardized nomenclature (46). Immunohistochemistry was performed by using paraffin-embedded decalcified sections (47) with a polyclonal first antibody raised against the human CB2-(20–33) peptide (Cayman Chemical, Ann Arbor, MI; catalog no. 101550). The same peptide (Cayman Chemical; catalog no. 301550) was used to block protein–antibody complex formation in control staining. The antibody is highly specific for the human and mouse CB2 and does not crossreact with CB1.

mRNA Analyses. Total RNA was prepared from primary osteoblastogenic cultures of stromal cells derived from femoral and tibial diaphyseal bone marrow of WT C57BL/6J mice grown in "osteogenic medium" containing ascorbic acid, β-glycerophosphate, and

dexamethasone (Sigma) as reported in ref. 14. Bone marrow-derived osteoclastogenic cultures were established from Ficoll-separated monocytic precursors and grown for 5–6 days in medium containing M-CSF and RANKL (R & D Systems) (48). In addition, mRNA was obtained from osteoclast-like RAW 264.7 cells grown for 7 days with or without RANKL supplementation. Real-time RT-PCR analysis was carried out by using Applied Biosystems Assay-on-Demand. Data were normalized to GAPDH. Assay ID: GAPDH, Mm99999915_g1; CB1, Mm00432621_s1; CB2, Mm00438286_m1; RUNX2, Mm00501578_m1; and TNSALP, Mm00475831_m1. RT-PCR analysis was carried out by using previously reported primers (49). RANKL and osteoprotegerin (OPG) mRNA expression was analyzed by RT-PCR in bone marrow-derived primary stromal cells grown in osteogenic medium by using the following primers: mouse RANKL, U: 5′-CGC TCT GTT CCT GTA CTT TCG AGC G-3′ and L, 5′-TCG TGC TCC CTC CTT TCA TCA GGT T-3′; mouse OPG, U, 5′-GGA AGG GCG TTA CCT GG-3′, and L, 5′-CTG CTC GCT CGA TTT GC-3′; and mouse β-actin, U, 5′-GAG ACC TTC AAC ACC CCA GCC-3′, and L, 5′-GGC CAT CTC TTG CTC GAA GTC-3′.

Determination of CFU-OB. Freshly isolated bone marrow cells from eight WT and five $CB2^{-/-}$ mice were seeded in 96-well plates, 10 wells per mouse, at 1×10^6 cells per well and cultured in osteogenic medium for 19 days. In the last 12 days, the medium was supplemented with 10^{-8} M HU-308 or vehicle solution (0.1% DMSO). CFU-OB was determined as the number of alizarin red S-positive colonies.

***In Vitro* Effect of HU-308.** The effects of HU-308 on osteoblastic cell growth and activity were studied in differentiating primary bone marrow-derived stromal cells (cultured as in *mRNA Analyses*), primary NeMCO prepared from 5-day-old mice by successive collagenase digestion (50), and MC3T3 E1 osteoblastic cells. The cells were initially incubated in osteogenic medium for 10–12 days, to allow for sufficient CB2 expression, followed by 2-h serum starvation. Ligands were dissolved in DMSO and further diluted to their final concentration by using tissue-culture medium. Cell counts and BrdUrd incorporation were determined after 48-h incubation in α-MEM supplemented with 4% BSA and ligand. The effect of HU-308 on osteoclast differentiation was measured in the osteoclastogenic system described above, supplemented with HU-308 dissolved initially in DMSO and diluted with medium. HU-308 was also tested in RAW 264.7 cells grown in medium with or without RANKL supplementation. BrdUrd incorporation was measured after 3 days. For osteoclast-like cell counts, 7-day cultures were fixed in ethanol and TRAP-stained.

Statistical Analyses. Differences between $CB2^{-/-}$ and WT mice were analyzed by *t* test. HU-308 and vehicle-treated OVX and sham-OVX mice were analyzed by ANOVA. When significant differences were indicated by ANOVA, group means were compared by using the Student–Newman–Keuls test for pairwise comparisons.

We thank M. Chorev for reading this manuscript, Z. Bar-Shavit for his contribution to the monocyte/osteoclast mRNA analysis, and O. Lahat for technical assistance. E.S. is affiliated with the David R. Bloom Center for Pharmacy, The Hebrew University School of Pharmacy (Jerusalem). This work was supported by National Institute on Drug Abuse Grant 9789 (to R.M.), Israel Science Foundation Grants 482/01 (to R.M.) and 4007/02-Bikura (to I.B. and E.S.), and Deutsche Forschungsgemeinschaft Grant SFB 645 (to M.K. and A.Z.). Purchase of the μCT system was supported in part by Israel Science Foundation Grant 9007/01 (to I.B.).

1. Rhee, M. H., Vogel, Z., Barg, J., Bayewitch, M., Levy, R., Hanus, L., Breuer, A. & Mechoulam, R. (1997) *J. Med. Chem.* **40,** 3228–3233.
2. Felder, C. C., Joyce, K. E., Briley, E. M., Mansouri, J., Mackie, K., Blond, O., Lai, Y., Ma, A. L. & Mitchell, R. L. (1995) *Mol. Pharmacol.* **48,** 443–450.
3. Herkenham, M., Lynn, A. B., Little, M. D., Johnson, M. R., Melvin, L. S., de Costa, B. R. & Rice, K. C. (1990) *Proc. Natl. Acad. Sci. USA* **87,** 1932–1936.
4. Zimmer, A., Zimmer, A. M., Hohmann, A. G., Herkenham, M. & Bonner, T. I. (1999) *Proc. Natl. Acad. Sci. USA* **96,** 5780–5785.
5. Munro, S., Thomas, K. L. & Abu-Shaar, M. (1993) *Nature* **365,** 61–65.
6. Julien, B., Grenard, P., Teixeira-Clerc, F., Van Nhieu, J. T., Li, L., Karsak, M., Zimmer, A., Mallat, A. & Lotersztajn, S. (2005) *Gastroenterology* **128,** 742–755.
7. Steffens, S., Veillard, N. R., Arnaud, C., Pelli, G., Burger, F., Staub, C., Zimmer, A., Frossard, J. L. & Mach, F. (2005) *Nature* **434,** 782–786.
8. Ducy, P., Amling, M., Takeda, S., Priemel, M., Schilling, A. F., Beil, F. T., Shen, J., Vinson, C., Rueger, J. M. & Karsenty, G. (2000) *Cell* **100,** 197–207.
9. Baldock, P. A., Sainsbury, A., Couzens, M., Enriquez, R. F., Thomas, G. P., Gardiner, E. M. & Herzog, H. (2002) *J. Clin. Invest.* **109,** 915–921.
10. Di Marzo, V., Goparaju, S. K., Wang, L., Liu, J., Batkai, S., Jarai, Z., Fezza, F., Miura, G. I., Palmiter, R. D., Sugiura, T. & Kunos, G. (2001) *Nature* **410,** 822–825.
11. Buckley, N. E., McCoy, K. L., Mezey, E., Bonner, T., Zimmer, A., Felder, C. C., Glass, M. & Zimmer, A. (2000) *Eur. J. Pharmacol.* **396,** 141–149.
12. David, V., Laroche, N., Boudignon, B., Lafage-Proust, M. H., Alexandre, C., Rüegsegger, P. & Vico, L. (2003) *J. Bone Miner. Res.* **18,** 1622–1631.
13. Ammann, P. & Rizzoli, R. (2003) *Osteoporos. Int.* **14,** S13–S18.
14. Frenkel, B., Capparelli, C., Van Auken, M., Baran, D., Bryan, J., Stein J. L., Stein, G. S. & Lian, J. B. (1997) *Endocrinology* **138,** 2109–2116.
15. Lian, J. B., Javed, A., Zaidi, S. K., Lengner, C., Montecino, M., van Wijnen, A. J., Stein, J. L. & Stein, G. S. (2004) *Crit. Rev. Eukaryot. Gene Expr.* **14,** 1–41.
16. Ross, R. A., Brockie, H. C. & Pertwee, R. G. (2000) *Eur. J. Pharmacol.* **401,** 121–130.
17. Chang, Y. H., Lee, S. T. & Lin, W. W. (2001) *J. Cell. Biochem.* **81,** 715–723.
18. Hanus, L., Breuer, A., Tchilibon, S., Shiloah, S., Goldenberg, D., Horowitz, M., Pertwee, R. G., Ross, R. A., Mechoulam, R. & Fride, E. (1999) *Proc. Natl. Acad. Sci. USA* **96,** 14228–14233.
19. Hanus, L., Abu-Lafi, S., Fride, E., Breuer, A., Vogel, Z., Shalev, D. E., Kustanovich, I. & Mechoulam, R. (2001) *Proc. Natl. Acad. Sci. USA* **98,** 3662–3665.
20. Rhee, M. H., Bayewitch, M., Avidor-Reiss, T., Levy, R. & Vogel, Z. (1998) *J. Neurochem.* **71,** 1525–1534.
21. Thomas, G. P., Baker, S. U., Eisman, J. A. & Gardiner, E. M. (2001) *J. Endocrinology* **170,** 451–460.
22. Wronski, T. J., Cintron, M. & Dann, L. M. (1988) *Calcif. Tissue Int.* **43,** 179–183.
23. Valk, P., Verbakel, S., Vankan, Y., Hol, S., Mancham, S., Ploemacher, R., Mayen, A., Lowenberg, B. & Delwel, R. (1997) *Blood* **90,** 1448–1457.
24. Sipe, J. C., Arbour, N., Gerber, A. & Beutler, E. (2005) *J. Leukocyte Biol.* **78,** 231–238.
25. Boyle, W. J., Simonet, W. S. & Lacey, D. L. (2003) *Nature* **423,** 337–342.
26. Elefteriou, F., Ahn, J. D., Takeda, S., Starbuck, M., Yang, X., Liu, X., Kondo, H., Richards, W. G., Bannon, T. W., Noda, M., *et al.* (2005) *Nature* **434,** 514–520.
27. Wei, S., Kitaura, H., Zhou, P., Ross, F. P. & Teitelbaum, S. L. (2005) *J. Clin. Invest.* **115,** 282–290.
28. Idris, A. I., van 't Hof, R. J., Greig, I. R., Ridge, S. A., Baker, D., Ross, R. A. & Ralston, S. H. (2005) *Nat. Med.* **11,** 774–779.
29. Puffenbarger, R. A., Boothe, A. C. & Cabral, G. A. (2000) *Glia* **29,** 58–69.
30. Molina-Holgado, F., Pinteaux, E., Moore, J. D., Molina-Holgado, E., Guaza, C., Gibson, R. M. & Rothwell, N. J. (2003) *J. Neurosci.* **23,** 6470–6474.
31. Bajayo, A., Goshen, I., Feldman, S., Csernus, V., Iverfeldt, K., Shohami, E., Yirmiya, R. & Bab, I. (2005) *Proc. Natl. Acad. Sci. USA* **102,** 12956–12961.
32. Kitazawa, R., Kimble, R. B., Vannice, J. L., Kung, V. T. & Pacifici, R. (1994) *J. Clin. Invest.* **94,** 2397–2406.
33. Sterin-Borda, L., Del Zar, C. F. & Borda, E. (2005) *Biochem. Pharmacol.* **69,** 1705–1713.
34. Vannacci, A., Gianini, L., Passani, M. B., Di Felice, A., Pierpaoli, S., Zagli, G., Fantappie, O., Mazzanti, R., Masini, E. & Mannaioni, P. F. (2004) *J. Pharmacol. Exp. Ther.* **311,** 256–264.
35. van 't Hof, R. J. & Ralston, S. H. (2001) *Immunology* **103,** 255–261.
36. Riggs B. L., Khosla, S. & Melton, L. J., III (1998) *J. Bone. Miner. Res.* **13**, 763–773.
37. Gonsiorek, W., Lunn, C., Fan, X., Narula, S., Lundell, D. & Hipkin, R. W. (2000) *Mol. Pharmacol.* **57,** 1045–1050.
38. Calvi, L. M., Sims, N. A., Hunzelman, J. L., Knight, M. C., Giovannetti, A., Saxton, J. M., Kronenberg, H. M., Baron, R. & Schipani, E. (2001) *J. Clin. Invest.* **107,** 277–286.
39. Wiren, K. M., Zhang, X. W., Toombs, A. R., Kasparcova, V., Gentile, M. A., Harada, S. & Jepsen, K. J. (2004) *Endocrinology* **145,** 3507–3522.
40. Karsak, M., Cohen-Solal, M., Freudenberg, J., Ostertag, A., Morieux, C., Kornak, U., Essig, J., Erxlebe, E., Bab, I., Kubisch, C., *et al.* (2005) *Hum. Mol. Genet.* **15,** 3389–3396.
41. Dreher, M. C. & Hayes, J. S. (1993) *West. J. Nurs. Res.* **15,** 216–229.
42. Beamer, W. G., Donahue, L. R., Rosen, C. J. & Baylink, D. J. (1996) *Bone* **18,** 397–403.
43. Müller, R. & Rüegsegger, P. (1997) *Stud. Health Technol. Inform.* **40,** 61–79.
44. Hildebrand, T., Laib, A., Müller, R., Dequeker, J. & Rüegsegger, P. (1999) *J. Bone Miner. Res.* **14,** 1167–1174.
45. Erlebacher, A. & Derynck, R. (1996) *J. Cell Biol.* **132,** 195–210.
46. Parfitt, A. M., Drezner, M. K., Glorieux, F. H., Kanis, J. A., Malluche, H., Meunier, P. J., Ott, S. M. & Recker, R. R. (1987) *J. Bone Miner. Res.* **2,** 595–610.
47. Ausubel, F. M. (1995) *Current Protocols in Molecular Biology* (Wiley Interscience, New York).
48. Zou, W., Schwartz, H., Endres, S., Hartmann, G. & Bar-Shavit, Z. (2002) *FASEB J.* **16,** 274–282.
49. Lee, S. F., Newton, C., Widen R., Friedman, H. & Klein, T. W. (2001) *Adv. Exp. Med. Biol.* **493,** 223–228.
50. Kato, M., Patel, M. S., Levasseur, R., Lobov, I., Chang, B. H., Glass, D. A., II, Hartmann, C., Li, L., Hwang, T. H., Brayton, C. F., *et al.* (2002) *J. Cell Biol.* **157**, 303–314.